

AUDIOX: A UNIFIED FRAMEWORK FOR ANYTHING-TO-AUDIO GENERATION

Anonymous authors

Paper under double-blind review

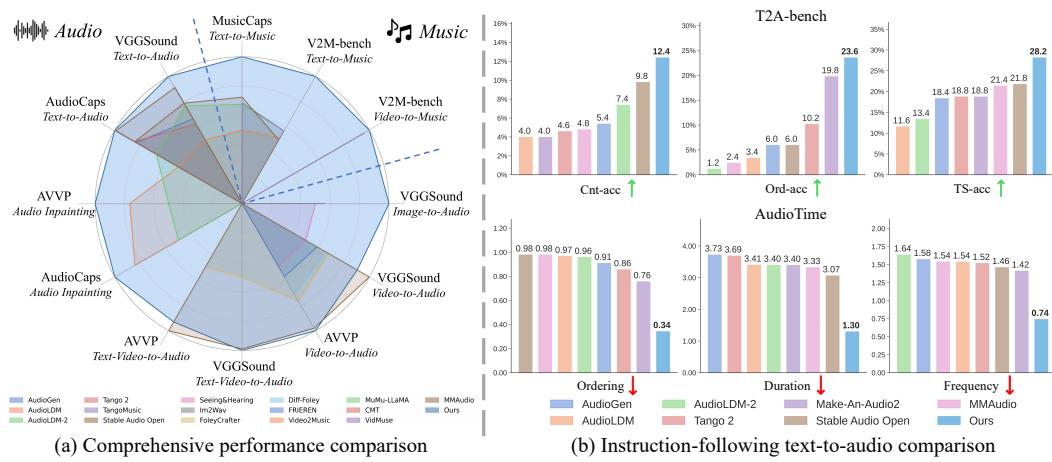


Figure 1: **Performance comparison of AudioX against baselines.** (a) Comprehensive comparison across multiple benchmarks via Inception Score. (b) Results on instruction-following benchmarks.

ABSTRACT

Audio and music generation based on flexible multimodal control signals is a widely applicable topic, with the following key challenges: 1) a unified multimodal modeling framework, and 2) large-scale, high-quality training data. As such, we propose AudioX, a unified framework for anything-to-audio generation that integrates varied multimodal conditions (*i.e.*, text, video, and audio signals) in this work. The core design in this framework is a Multimodal Adaptive Fusion module, which enables the effective fusion of diverse multimodal inputs, enhancing cross-modal alignment and improving overall generation quality. To train this unified model, we construct a large-scale, high-quality dataset, IF-caps, comprising over 7 million samples curated through a structured data annotation pipeline. This dataset provides comprehensive supervision for multimodal-conditioned audio generation. We benchmark AudioX against state-of-the-art methods across a wide range of tasks, finding that our model achieves superior performance, especially in text-to-audio and text-to-music generation. These results demonstrate our method is capable of audio generation under multimodal control signals, showing powerful instruction-following potential¹. We will release the code, model, and dataset.

1 INTRODUCTION

In recent years, audio generation, especially for sound effects and music, has emerged as a crucial element in multimedia creation, showing practical values in enhancing user experiences across a

¹Generated samples can be found in https://anonymous.4open.science/w/audiox_gen/

054 wide range of applications. For example, in social media, film production, and video games, sound
 055 effects and music significantly intensify emotional resonance and engagement with the audience.
 056 The ability to create high-quality audio not only enriches multimedia content but also opens up new
 057 avenues for creative expression.

058 However, the manual production of audio is time-consuming and requires specialized skills, pre-
 059 senting a compelling research opportunity to automate audio generation. Despite notable advance-
 060 ments (Liu et al., 2023; Copet et al., 2024; Wang et al., 2024), the field has predominantly focused
 061 on specialized models with constrained inputs and outputs. These models often operate with a
 062 single conditioning modality, such as text-to-audio or video-to-audio, and are typically restricted
 063 to a single output domain, like generating either sound effects (Cheng et al., 2025) or music (Tian
 064 et al., 2025) exclusively. While a recent trend towards unification is emerging, with some pioneering
 065 works accommodating multiple inputs (Polyak et al., 2024; Zhang et al., 2024), they often lack the
 066 flexibility to support diverse modal combinations and exhibit weak instruction-following abilities.
 067 As a result, the potential of unified models still remains underexplored. We find that a major factor
 068 behind these limitations is the scarcity of high-quality, multimodal data suitable for training unified
 069 systems. Existing datasets are often task-specific, typically providing supervision for only one con-
 070 ditioning modality, such as text-to-audio (Kim et al., 2019), video-to-audio (Chen et al., 2020), or
 071 video-to-music (Tian et al., 2025). This lack of datasets with diverse and combinable control signals
 072 has significantly hindered the development and training of unified models.

073 To this end, we propose a unified framework termed AudioX for anything-to-audio generation. We
 074 observe that Transformer-based works (Wu et al., 2023a; Liu et al., 2024b; Lin et al., 2023) have ef-
 075 fectively tackled multi-modal alignment, and we build on this success by incorporating Transformer-
 076 based methods into our framework for multi-modal condition handling. Furthermore, diffusion mod-
 077 els have increasingly become leading-edge techniques in the field of high-quality audio and music
 078 generation (Evans et al., 2024a;b), outperforming next-token prediction in terms of audio fidelity
 079 (Evans et al., 2024a; Majumder et al., 2024). Therefore, we mainly build on Diffusion Transformer
 080 (DiT) to unify multimodal conditions and generate high-fidelity audio. To further enhance multi-
 081 modal representation learning and alignment, we introduce a lightweight Multimodal Adaptive
 082 Fusion module that adaptively weights and aligns conditioning modalities before fusion, enabling
 083 stronger cross-modal control and yielding significant improvements in generation quality.

083 To support the training of a unified model, we designed a pipeline using structured annotation and
 084 data augmentation to build IF-caps (Instruction-Following), a large-scale, high-quality multimodal
 085 dataset. The dataset serves as a robust foundation for our approach, containing over 1.3 million
 086 general audio samples and 5.7 million music samples. Training on this large-scale, fine-grained
 087 dataset allows our model to handle flexible multimodal conditions and generate diverse audio genres,
 088 including music and sound effects. Consequently, AudioX enables a range of tasks, including text-
 089 to-audio generation, video-to-audio generation, audio inpainting, and text-guided music completion.

090 With this unified design and trained on our large-scale dataset, our model demonstrates exceptional
 091 performance and strong instruction-following capabilities. To validate our model’s capabilities, we
 092 benchmark it against state-of-the-art methods across a comprehensive suite of tasks and established
 093 benchmarks. In addition, to rigorously evaluate its instruction-following ability on T2A tasks, we
 094 construct a new benchmark, T2A-bench. As demonstrated in Sec. 5.3, AudioX achieves state-of-
 095 the-art or comparable results across multiple benchmarks and various tasks, while substantially out-
 096 performing prior methods in instruction-following capabilities. A notable finding from our unified
 097 training approach is that we observe a *cross-modal regularization effect* under unified training:
 098 improving the quality and granularity of textual supervision reduces alignment noise and leads to
 099 better modality alignment, which jointly improves performance across conditioning modalities (see
 100 Sec. 5.4). This observation provides empirical insight for future multimodal audio generation.

101 In summary, the main contributions of this work are as follows: 1) We propose AudioX, a unified
 102 framework for anything-to-audio generation that overcomes the limitations of constrained inputs and
 103 outputs. The proposed framework supports audio and music generation from varied multi-modal
 104 conditions, contributing to a new insight into studying generalist models for audio generation.

105 2) To overcome data scarcity for unified training, we design a data curation pipeline and construct
 106 a large-scale, high-quality dataset, IF-caps, containing over 7 million samples with fine-grained
 107 annotations.

108 3) We conduct comprehensive experiments on a wide array of tasks, systematically benchmarking
 109 state-of-the-art methods categorized by their input modalities and output domains. Our extensive ex-
 110 periments demonstrate our model’s strong multi-task capabilities and superior instruction-following
 111 ability.

112

113

2 RELATED WORK

114

115

116 Audio and music generation. Recent advances in deep generative models have greatly broadened
 117 the scope of audio and music synthesis. However, most existing methods remain confined to a single
 118 modality or support only limited types of conditioning. For instance, *text-to-audio* approaches (Liu
 119 et al., 2023; Kreuk et al., 2022; Ghosal et al., 2023; Majumder et al., 2024; Evans et al., 2024a;b;
 120 Jiang et al., 2025; Huang et al., 2023) focus on generating diverse soundscapes from textual prompts,
 121 while *text-to-music* systems (Copet et al., 2024; Liu et al., 2023; 2024a; Ghosal et al., 2023; Ziv et al.,
 122 2024b) specialize in composing coherent musical pieces. Separate lines of work tackle tasks like
 123 *audio inpainting* (Liu et al., 2023; 2024a), primarily with text conditioning. Meanwhile, *video-to-*
 124 *audio* methods (Zhang et al., 2024; Luo et al., 2024; Wang et al., 2024; Polyak et al., 2024; Chen
 125 et al., 2024) typically generate foley or environmental sounds synchronized to visual cues. Some of
 126 these also incorporate text for additional context, thereby bridging visual and textual modalities. Be-
 127 yond sound effects, *video-to-music* approaches (Kang et al., 2024; Liu et al., 2024c; Di et al., 2021;
 128 Tian et al., 2025; Li et al., 2024b; Lin et al., 2024; Li et al., 2024a) align musical compositions with
 129 the visual content to enhance narrative depth in multimedia applications. Despite these advances,
 130 current frameworks often specialize in only one modality or rely on a limited set of input conditions,
 131 hindering multi-task adaptation and restricting their ability to scale or transfer knowledge across
 132 related tasks. In contrast, our *unified* approach supports both audio and music generation for a broad
 133 range of input conditions—including text, video, and audio—all within a single framework.

134

135

136

137

138

139

140

141

142

143

144

145

146

147

148

149

150

151

152 Audio Datasets. While substantial research efforts
 153 have led to the creation of valuable datasets for spe-
 154 cific tasks like text-to-audio (Kim et al., 2019; Mei
 155 et al., 2024; Drossos et al., 2020; Wu et al., 2023b),
 156 text-to-music (Copet et al., 2024; Liu et al., 2024c;
 157 Ramires et al., 2020), video-to-audio (Chen et al.,
 158 2020; Hershey et al., 2021; Tian et al., 2020), and
 159 video-to-music (Tian et al., 2025; Zhou et al., 2025),
 160 their utility for training a generalist unified model
 161 remains limited. These resources are typically con-
 162 strained to a single conditioning modality and a nar-
 163 row output domain (e.g., only sound effects or only
 164 music). This fragmentation of data has significantly
 165 hindered progress towards developing more versa-
 166 tile and robust systems. To overcome this critical
 167 data scarcity, we introduce a large-scale, multimodal
 168 dataset constructed via a novel annotation and aug-
 169 mentation pipeline, specifically designed to provide
 170 the comprehensive supervision required for unified
 171 audio and music generation.

172

173

174

175

176

177

178

179

180

181

182

183

184

185

186

187

188

189

190

191

192

193

194

195

196

197

198

199

200

201

202

203

204

205

206

207

208

209

210

211

212

213

214

215

216

217

218

219

220

221

222

223

224

225

226

227

228

229

230

231

232

233

234

235

236

237

238

239

240

241

242

243

244

245

246

247

248

249

250

251

252

253

254

255

256

257

258

259

260

261

262

263

264

265

266

267

268

269

270

271

272

273

274

275

276

277

278

279

280

281

282

283

284

285

286

287

288

289

290

291

292

293

294

295

296

297

298

299

300

301

302

303

304

305

306

307

308

309

310

311

312

313

314

315

316

317

318

319

320

321

322

323

324

325

326

327

328

329

330

331

332

333

334

335

336

337

338

339

340

341

342

343

344

345

346

347

348

349

350

351

352

353

354

355

356

357

358

359

360

361

362

363

364

365

366

367

368

369

370

371

372

373

374

375

376

377

378

379

380

381

382

383

384

385

386

387

388

389

390

391

392

393

394

395

396

397

398

399

400

401

402

403

404

405

406

407

408

409

410

411

412

413

414

415

416

417

418

419

420

421

422

423

424

425

426

427

428

429

430

431

432

433

434

435

436

437

438

439

440

441

442

443

444

445

446

3 DATASET PROCESS

Existing audio datasets often lack the high-quality, multimodal conditioning signals necessary to train versatile, unified models. To address this gap, we designed an effective annotation pipeline that processes existing video datasets (Chen et al., 2020; Hershey et al., 2021; Tian et al., 2025), allowing us to construct IF-caps, a large-scale dataset with diverse, multi-modal conditions. Our pipeline, as shown in Fig. 2, operates as follows: **First**, we employ a powerful multimodal LLM (Gemini 2.5 Pro) to generate a comprehensive set of initial annotations **by processing the audio track of** each 10-second video-audio clip. These annotations consist of a holistic global caption and a set of structured fields. For general audio, these fields include sound event classification and count; for music, they specify attributes like genre and instrumentation. **Then**, since using the resource-intensive Gemini model for the entire dataset is costly, we leverage the open-source Qwen2-Audio (Chu et al., 2024) model to augment these structured fields at a large scale. Conditioned on both the initial annotations and the raw audio, the model generates varied captions, enhancing data diversity while managing costs. **Finally**, this process yields comprehensive, fine-grained captions for approximately 1.3 million video-audio clips and 5.7 million video-music clips. The diversity of our curated dataset is highlighted by the word clouds in Fig. 3. More details and samples of our annotated data are provided in the Appendix A.1.2.

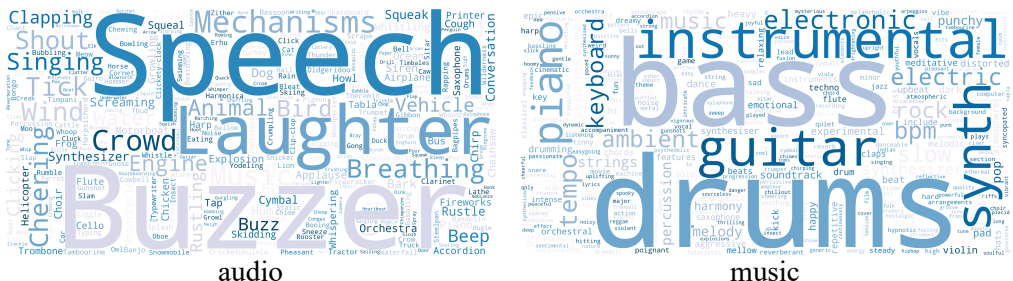


Figure 3: Word clouds for our curated dataset, illustrating the diversity of terms for the general audio (left) and music (right) domains.

4 METHOD

4.1 MODEL DESIGN

Our framework, AudioX, as shown in Fig. 4, is built upon a DiT backbone designed for high-fidelity audio synthesis. Given video \mathbf{X}_v , text \mathbf{X}_t , and audio \mathbf{X}_a , each modality is passed through corresponding specialized encoders. To capture the temporal dynamics, the resulting video and audio features are then processed by a temporal transformer. Finally, the features from all three modalities are mapped through a projection head to produce the domain-specific embeddings (\mathbf{H}_v , \mathbf{H}_t , \mathbf{H}_a). These embeddings are then fused into a unified condition embedding, which is ultimately passed to the Diffusion Transformer to guide the generation process.

A key challenge in training a unified model is that signals from different modalities can interfere with each other, making effective fusion and well-aligned conditioning critical. To address this, we introduce the lightweight **Multimodal Adaptive Fusion (MAF)** module. As shown in Fig. 4 (right), the MAF module operates as follows: *First*, the initial feature embeddings from each modality are fed into *gates*, which filter and reweight them to suppress noise and retain the most informative cues. *Next*, the gated embeddings are concatenated and attended by *learnable queries* via cross-attention. These queries are organized into three modality-specific sets, acting as experts to assess and aggregate evidence across the different data streams. *Finally*, a *self-attention* layer consolidates this aggregated context, and the refined information is dispatched back to the modality paths via residual updates. This process yields calibrated, modality-specific outputs which are then concatenated to form the final multimodal condition embedding, \mathbf{H}_c :

$$\tilde{\mathbf{H}}_v, \tilde{\mathbf{H}}_t, \tilde{\mathbf{H}}_a = \text{MAF}(\mathbf{H}_v, \mathbf{H}_t, \mathbf{H}_a), \quad \mathbf{H}_c = \text{Concat}\left(\tilde{\mathbf{H}}_v, \tilde{\mathbf{H}}_t, \tilde{\mathbf{H}}_a\right). \quad (1)$$

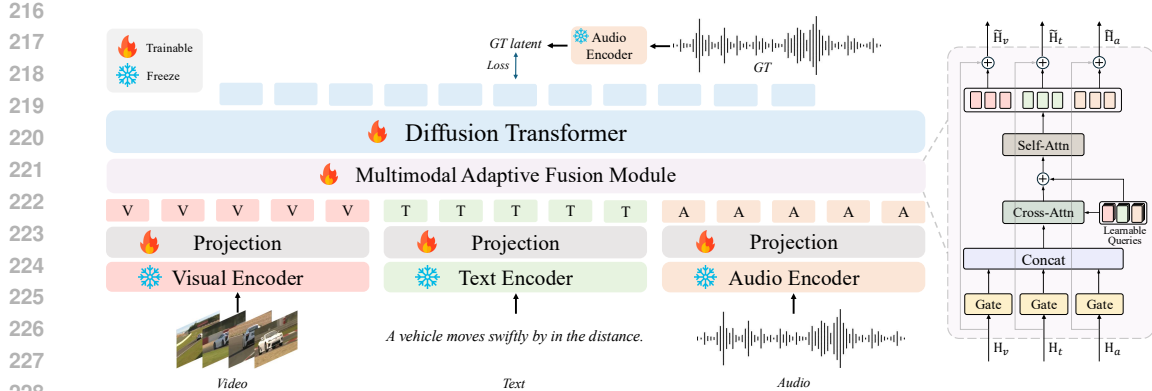


Figure 4: **The AudioX Framework.** Specialized encoders process diverse modalities, and a MAF module unifies these signals into a conditioning embedding H_c . The DiT backbone processes the noisy latent input z_t , conditioning on H_c via cross-attention to generate high-quality audio and music. (z_t and H_c notations are omitted for visual clarity).

This final embedding, along with a diffusion timestep t , is what conditions the DiT backbone for the final audio synthesis. As we demonstrate in our ablation studies (Sec. 5.4), the MAF module is essential for reducing cross-modal interference while improving both the overall generation quality on multimodal tasks and the model’s instruction-following capabilities.

4.2 TRAINING

The objective of the training process is to effectively integrate multimodal inputs and optimize the DiT model for generating high-quality audio or music through a robust diffusion and denoising framework. The details of the training data are provided in Table A.1 in the Appendix. During training, for each pair $(\mathbf{X}_v, \mathbf{X}_t, \mathbf{X}_a | \mathbf{A})$, where \mathbf{A} is the ground truth we aim to generate, if the pair lacks video or audio modality input, we use zero-padding to fill the missing modality. If it lacks text modality input, we substitute with natural language descriptions, such as “Generate music for the video.” for the video-to-music generation task. For the tasks of audio inpainting and music completion, the audio modality input is required. In audio inpainting, \mathbf{X}_a is a masked version of the ground truth audio \mathbf{A} , and the model’s objective is to fill in the masked sections. For music completion, \mathbf{X}_a is the preceding music segment of \mathbf{A} , and the model aims to generate the subsequent music segment of \mathbf{X}_a .

Diffusion process. The DiT model processes the multimodal embedding \mathbf{H}_c in the latent space through a denoising diffusion process. Initially, the ground truth \mathbf{A} is encoded using an encoder \mathcal{E} , which projects \mathbf{A} into the latent space, yielding the latent representation $\mathbf{z} = \mathcal{E}(\mathbf{A})$. The data then undergoes a forward diffusion process, producing noisy latent states at each timestep t .

The forward diffusion is defined as a Markov process over T timesteps, where the latent state at timestep t is produced based on the latent state at $t-1$:

$$q(\mathbf{z}_t | \mathbf{z}_{t-1}) = \mathcal{N}(\mathbf{z}_t; \sqrt{1 - \beta_t} \mathbf{z}_{t-1}, \beta_t \mathbf{I}), \quad (2)$$

where β_t represents the predefined variance at timestep t , and \mathcal{N} denotes a Gaussian distribution. The forward diffusion process gradually adds noise to the latent state.

The reverse denoising process involves training a transformer network ϵ_θ to gradually remove noise at each timestep and reconstruct the clean data. The reverse process is modeled as follows:

$$p_\theta(\mathbf{z}_{t-1} | \mathbf{z}_t) = \mathcal{N}(\mathbf{z}_{t-1}; \mu_\theta(\mathbf{z}_t, t, \mathbf{H}_c), \Sigma_\theta(\mathbf{z}_t, t, \mathbf{H}_c)), \quad (3)$$

where μ_θ and Σ_θ are the predicted mean and covariance of the reverse diffusion, conditioned on \mathbf{z}_t , t , and \mathbf{H}_c . These parameters define the Gaussian distribution from which \mathbf{z}_{t-1} is sampled.

The denoiser network ϵ_θ takes as input the noisy latent state \mathbf{z}_t , timestep t , and the multimodal condition embedding \mathbf{H}_c . The goal is to minimize the noise estimation error at each timestep,

270 which is formulated as:

$$\min_{\theta} \mathbb{E}_{t, \mathbf{z}_t, \epsilon} \|\epsilon - \epsilon_{\theta}(\mathbf{z}_t, t, \mathbf{H}_c)\|_2^2, \quad (4)$$

273 where ϵ is the simulated noise at timestep t , and $\epsilon_{\theta}(\mathbf{z}_t, t, \mathbf{H}_c)$ is the predicted noise from the model.
 274 The training objective is to minimize the mean squared error between the simulated and predicted
 275 noise across all timesteps.

276 By training the DiT model in this manner, we effectively unify multimodal inputs into a latent space,
 277 enabling the generation of high-quality audio or music that is coherent and aligned with the input
 278 conditions.

281 5 EXPERIMENTS

283 In this section, we provide the implementation details of our experiments and conduct extensive
 284 evaluations. These assessments comprehensively measure the effectiveness of our proposed method
 285 from both subjective and objective viewpoints. The evaluations aim to offer valuable insights into
 286 the generation of audio and music from various inputs.

288 5.1 IMPLEMENTATION DETAILS

290 For encoding the visual features, we use CLIP-ViT-B/32 (Radford et al., 2021) to extract video
 291 frame features at a rate of 5 fps, and Synchformer (Iashin et al., 2024) to extract synchronization
 292 features at 25 fps. The CLIP and Synchformer features are fused via addition. The text inputs
 293 are encoded using T5-base (Raffel et al., 2020), while the audio is encoded and decoded using an
 294 audio Autoencoder (Evans et al., 2024b). The model has a total of 2.4B parameters (1.1B trainable).
 295 Our proposed MAF module constitutes only 60M of these parameters, highlighting its lightweight
 296 nature. The DiT model, consisting of 24 layers, uses a pretrained model from (Evans et al., 2024b).

297 The training process uses the AdamW optimizer with a base learning rate of 1e-5, weight decay of
 298 0.001, and a learning rate scheduler incorporating exponential ramp-up and decay phases. To im-
 299 prove inference stability, we maintain an exponential moving average of the model weights. Training
 300 is conducted on three clusters of NVIDIA H800 GPUs, each with 80GB of memory, requiring ap-
 301 proximately 4k GPU hours in total. The batch size is set to 48. During inference, we perform 250
 302 steps using classifier-free guidance with a scale of 7.0. Please refer to Appendix A.1.1 for further
 303 details on our training and evaluation datasets.

304 5.2 EVALUATION METRICS

306 To provide a comprehensive assessment of our model, we employ a suite of objective and subjective
 307 metrics. Further details for each metric are provided in the Appendix A.2.

309 **Objective Evaluation.** For overall audio quality and semantic alignment, we use several estab-
 310 lished metrics. These include: Kullback-Leibler Divergence (KL); Inception Score (IS); Fréchet
 311 Distance (FD) with PANNs embeddings (Kong et al., 2020); Fréchet Audio Distance (FAD) with
 312 VGGish embeddings (Hershey et al., 2017); Production Complexity (PC) and Production Quality
 313 (PQ) (Tjandra et al., 2025). As a prompt-free metric for both quality and diversity, we chose IS for
 314 the unified comparison in Fig. 1. For alignment, we use the CLAP score (Wu et al., 2023b) for text
 315 inputs and the Imagebind AV score (Girdhar et al., 2023) for video inputs. To assess the model’s
 316 instruction-following capabilities in T2A, we report metrics on two benchmarks. On our proposed
 317 T2A-bench (detailed in Appendix A.3), we measure category, count, ordering, and timestamp accu-
 318 racy (Cat-acc, Cnt-acc, Ord-acc, TS-acc). On AudioTime (Xie et al., 2025), we use its established
 319 metrics for Ordering, Duration, Frequency, and Timestamp.

321 **Subjective Evaluation.** We conducted a formal user study with 10 professional audio experts to
 322 evaluate the subjective quality of our generated samples against baselines. The study followed the
 323 established methodologies of prior work (Kreuk et al., 2022; Liu et al., 2023), where experts rated
 anonymized samples from 1 to 100 on Overall Quality (OVL) and Relevance (REL) to the prompt.

324
 325 **Table 1: Performance evaluation across various tasks and datasets.** Task abbreviations are: T2A
 326 (Text-to-Audio), V2A (Video-to-Audio), TV2A (Text-and-Video-to-Audio), T2M (Text-to-Music),
 327 V2M (Video-to-Music), and TV2M (Text-and-Video-to-Music). For alignment (Align.), we use the
 328 CLAP score for text and the Imagebind AV score for video inputs.

Dataset	Method	Task	KL ↓	IS ↑	FD ↓	FAD ↓	PC ↑	PQ ↑	Align.↑
AudioCaps	AudioGen(Kreuk et al., 2022)	T2A	1.39	10.22	13.29	1.72	3.26	5.25	0.27
	AudioLDM-L-Full(Liu et al., 2023)	T2A	2.00	6.51	37.27	8.37	2.82	5.67	0.20
	AudioLDM-2-Large(Liu et al., 2024a)	T2A	1.49	8.46	26.34	1.97	2.86	5.77	0.22
	Tango 2(Majumder et al., 2024)	T2A	1.11	10.37	12.22	3.20	3.63	5.82	0.36
	Stable Audio Open(Evans et al., 2024b)	T2A	2.01	10.37	29.01	3.15	2.77	6.16	0.21
	MAGNET-large(Ziv et al., 2024a)	T2A	1.62	7.46	24.88	2.99	3.25	5.15	0.15
	MMAudio(Cheng et al., 2025)	T2A	1.35	12.03	12.63	4.71	3.06	5.64	0.30
VGGSound	AudioX	T2A	1.27	12.48	11.51	1.59	3.32	5.80	0.30
	AudioGen(Kreuk et al., 2022)	T2A	2.16	11.09	15.94	2.48	3.30	5.45	0.29
	AudioLDM-L-Full(Liu et al., 2023)	T2A	2.41	6.52	31.15	7.05	2.93	5.99	0.27
	AudioLDM-2-Large(Liu et al., 2024a)	T2A	2.10	13.86	16.32	2.05	2.95	6.35	0.30
	Tango 2(Majumder et al., 2024)	T2A	2.31	10.00	22.96	3.47	3.93	5.99	0.29
	Stable Audio Open(Evans et al., 2024b)	T2A	2.36	14.45	26.00	2.60	2.64	6.53	0.33
	MAGNET-large(Ziv et al., 2024a)	T2A	2.03	8.53	22.17	2.74	3.65	5.25	0.26
AVVP	MMAudio(Cheng et al., 2025)	T2A	2.17	17.83	11.52	2.50	3.02	6.12	0.32
	AudioX	T2A	1.74	19.58	9.01	1.33	3.34	6.31	0.33
	Seeing&Hearing(Xing et al., 2024)	V2A	2.58	5.15	27.21	5.23	3.42	5.33	0.36
	FoleyCrafter(Zhang et al., 2024)	V2A	2.39	8.70	17.68	2.23	3.31	5.99	0.27
	Diff-Foley(Luo et al., 2024)	V2A	3.01	8.35	56.54	5.89	2.57	5.85	0.20
	FRIEREN(Wang et al., 2024)	V2A	2.58	6.91	50.88	3.13	2.98	6.06	0.20
	MMAudio(Cheng et al., 2025)	V2A	1.97	14.95	6.18	2.04	3.38	5.91	0.35
MusicCaps	AudioX	V2A	2.21	12.60	7.84	1.28	3.49	6.21	0.26
	FoleyCrafter(Zhang et al., 2024)	TV2A	1.94	11.32	19.16	2.13	3.38	6.06	0.26
	MMAudio(Cheng et al., 2025)	TV2A	1.51	17.79	6.60	2.20	3.31	5.99	0.33
	AudioX	TV2A	1.48	17.91	6.97	1.06	3.46	6.29	0.26
	Seeing&Hearing(Xing et al., 2024)	V2A	2.30	4.02	40.38	8.66	3.64	5.16	0.35
	FoleyCrafter(Zhang et al., 2024)	V2A	2.13	6.46	28.68	3.77	3.25	5.87	0.28
	Diff-Foley(Luo et al., 2024)	V2A	3.14	5.97	76.96	10.95	2.55	5.71	0.16
V2M-bench	FRIEREN(Wang et al., 2024)	V2A	2.73	4.71	66.46	6.49	3.08	5.88	0.17
	MMAudio(Cheng et al., 2025)	V2A	1.22	8.40	13.51	3.25	3.55	5.89	0.34
	AudioX	V2A	1.89	8.60	17.2	2.24	3.65	6.09	0.28
	FoleyCrafter(Zhang et al., 2024)	TV2A	1.81	6.22	26.76	2.85	3.62	5.60	0.27
	MMAudio(Cheng et al., 2025)	TV2A	1.74	9.52	14.18	2.74	3.64	5.81	0.34
	AudioX	TV2A	1.88	9.03	16.33	2.38	3.65	6.04	0.28
	MusicGen(Copet et al., 2024)	T2M	1.43	2.24	25.40	4.55	5.19	7.16	0.18
V2M-bench	AudioLDM-L-Full(Liu et al., 2023)	T2M	1.45	2.49	34.44	6.34	4.72	6.10	0.22
	AudioLDM-2-Large(Liu et al., 2024a)	T2M	1.26	2.84	15.61	2.80	5.22	6.70	0.23
	TangoMusic(Ghosal et al., 2023)	T2M	1.13	2.86	15.00	1.88	5.57	7.06	0.23
	Stable Audio Open(Evans et al., 2024b)	T2M	1.51	2.94	36.33	3.23	3.91	7.18	0.23
	MAGNET-large(Ziv et al., 2024a)	T2M	1.32	1.98	23.88	4.24	5.84	6.71	0.19
	AudioX	T2M	0.96	3.55	9.76	1.47	5.21	6.70	0.24
	MusicGen(Copet et al., 2024)	T2M	0.76	1.31	40.59	3.25	5.57	7.43	0.14
V2M-bench	AudioLDM-L-Full(Liu et al., 2023)	T2M	0.72	1.37	36.63	2.97	5.08	7.01	0.16
	AudioLDM-2-Large(Liu et al., 2024a)	T2M	0.62	1.46	25.80	1.63	5.57	6.90	0.14
	TangoMusic(Ghosal et al., 2023)	T2M	0.72	1.46	38.19	2.43	5.78	7.46	0.14
	Stable Audio Open(Evans et al., 2024b)	T2M	0.72	1.34	42.02	2.72	4.36	7.72	0.17
	MAGNET-large(Ziv et al., 2024a)	T2M	0.60	1.26	34.24	3.15	5.89	7.04	0.17
	AudioX	T2M	0.47	1.50	19.62	1.68	5.91	7.12	0.14
	Video2Music(Kang et al., 2024)	V2M	1.78	1.01	144.88	18.72	3.34	8.14	0.14
364	MuMu-LLaMA(Liu et al., 2024c)	V2M	1.00	1.25	52.25	5.10	5.60	7.97	0.18
	CMT(Di et al., 2021)	V2M	1.22	1.24	85.70	8.64	4.98	8.20	0.12
	VidMuse(Tian et al., 2025)	V2M	0.73	1.32	29.95	2.46	5.88	6.89	0.20
	AudioX	V2M	0.70	1.37	24.01	1.67	5.24	7.04	0.23
	AudioX	TV2M	0.45	1.52	18.64	1.44	5.42	7.24	0.22

5.3 MAIN RESULTS

This work introduces a unified model capable of generating audio and music from flexible combinations of video, text, and audio inputs. Through extensive experimentation, we benchmark our model against SOTA specialist models across all supported tasks. Results demonstrate that our single model consistently achieves SOTA or highly competitive performance on the majority of metrics.

Audio generation. Results of our audio generation are in Table 1, which includes the outcomes of generating audio or music from any combination of video and text modalities. The upper part of the table presents the audio generation tasks, while the lower part displays the music generation tasks.

For text-to-audio generation, we evaluate on the AudioCaps (Kim et al., 2019) and VGGSound (Chen et al., 2020) datasets. On AudioCaps, our model achieves SOTA performance, while on VGGSound, the advantage is even more pronounced. This demonstrates that our model is a powerful text-to-audio generator. Furthermore, both our model and baseline results on VGGSound confirm the effectiveness of our curated caption data. For video-to-audio generation, we experiment on

VGGSound and AVVP (Tian et al., 2020), AVVP is an out-of-domain test dataset for all methods. Our model achieves results comparable to SOTA on both VGGSound and AVVP, proving that it is not only a strong video-to-audio generator but also exhibits excellent generalization on out-of-domain datasets. For audio generation conditioned on both text and video, we benchmark against the strong baselines FoleyCrafter (Zhang et al., 2024) and MMAudio (Cheng et al., 2025), achieving results that are comparable to them. We find that when both text and video inputs are provided, the model effectively integrates the information from both modalities to generate better results.

The bottom part of Table 1 shows the results of music generation tasks. On the V2M dataset (Tian et al., 2025), we evaluate text-to-music, video-to-music, and video-and-text-to-music. The text-to-music task is additionally evaluated on the MusicCaps (Copet et al., 2024) dataset. Our model achieves SOTA performance across these tasks, demonstrating its effectiveness in generating high-quality music conditioned on diverse inputs.

Table 2: Evaluation of instruction-following T2A ability on the T2A-bench and AudioTime.

Method	T2A-bench				AudioTime			
	Cat-acc ↑	Cnt-acc ↑	Ord-acc ↑	TS-acc ↑	Ordering ↓	Duration ↓	Frequency ↓	Timestamp↑
AudioGen	24.40	5.40	6.00	18.40	0.91	3.73	1.58	0.54
AudioLDM	18.60	4.00	3.40	11.60	0.97	3.41	1.54	0.41
AudioLDM-2	20.10	7.40	1.20	13.40	0.96	3.40	1.64	0.54
Tango 2	25.20	4.60	10.20	18.80	0.86	3.70	1.52	0.61
Make-An-Audio2	32.40	4.00	19.80	18.80	0.76	3.40	1.42	0.56
Stable Audio Open	31.20	9.80	6.00	21.80	0.98	3.07	1.46	0.53
MMAudio	26.60	4.80	2.40	21.40	0.98	3.33	1.54	0.50
AudioX	34.20	12.40	23.60	28.20	0.34	1.30	0.74	0.81

Instruction-following text-to-audio generation. As shown in Figure 1 and Table 2, AudioX substantially outperforms all baselines in tasks requiring fine-grained control. On our T2A-bench, AudioX demonstrates a commanding lead across all dimensions, from category generation to count and temporal control. For instance, it surpasses the temporally-enhanced Make-An-Audio2 baseline in Ord-acc. This advantage is reaffirmed on the AudioTime benchmark. We also note that the performance trends between AudioTime’s Ordering metric and our Ord-acc are consistent across all models, which helps validate the design of our benchmark for evaluating temporal adherence. Furthermore, an insight from these comparisons is that high audio fidelity does not necessarily correlate with instruction-following prowess. For instance, Tango2, despite its high-quality synthesis, delivers only moderate performance on these control-focused metrics. Collectively, these results underscore our model’s superior fine-grained control, setting a new standard for controllable T2A generation.

User study. We conducted a user study to evaluate the quality of the generated audio and music. We randomly selected 25 samples for each audio generation task, including T2A, T2M, V2A, and V2M. 10 audio experts are asked to rate the quality of the generated audio and music. The results are shown in Fig. A.2 in the Appendix. The evaluation shows that our model achieves subjective SOTA performance in terms of OVL and REL scores in most tasks, indicating high user satisfaction.

To further demonstrate the versatility of our model, we present results for additional tasks, including audio inpainting, music completion, and image-to-audio generation, in Appendix A.4.1. The results further underscore our model’s strong performance and broad applicability across a variety of audio generation tasks.

5.4 ABLATION STUDY

In this section, we conduct a series of ablation studies to investigate the contribution of our key design choices. We systematically validate the efficacy of our data curation strategy and the architectural integrity of the proposed MAF module. An additional ablation study on the impact of different conditioning modalities is detailed in Appendix A.4.2.

Efficacy of data curation strategy.

To verify the impact of our data curation strategy, we evaluate models trained on different textual supervision sources (Table 3): 1) **Labels**: using raw class labels from the source datasets; 2) **AudioSetCaps**: using captions from a recent concurrent dataset (Bai et al., 2025); 3) **QwenCap**: using captions generated directly by Qwen2-Audio; 4) **GeminiCap**: using only the initial annotations generated by Gemini 2.5 Pro; and 5) **GeminiCap-aug**: our full pipeline. The results show

432 that *GeminiCap-aug* outperforms all baselines, including the external *AudioSetCaps* dataset and
 433 the single-stage generation methods. It not only achieves the best scores on general-purpose tasks
 434 (*T2A*, *V2A*, *TV2A*) but also enhances the model’s instruction-following capabilities. Collectively,
 435 these results validate the superior quality of our constructed dataset and the effectiveness of the
 436 *proposed two-stage curation pipeline*. Notably, we observe that the benefits of high-quality textual
 437 supervision are not limited to text-to-audio generation. The marked improvement in the *V2A* task
 438 provides strong empirical evidence of a *cross-modal regularization effect*. This insight leads to a
 439 crucial conclusion for future work: high-quality textual data should be viewed not only as an input,
 440 but also as an effective strategy for building more capable and robust multimodal models.

441
 442 **Table 3: Ablation study on data curation strategies.** We compare our model’s performance when
 443 trained with captions from different sources. The results show a clear trend of improvement with
 444 higher-quality data. Our full pipeline (*GeminiCap-aug*) not only achieves the best performance
 445 on all general tasks (*T2A*, *V2A*, *TV2A*) but is also essential for enabling fine-grained control.

Caption Method	Instruction-following T2A			T2A		V2A		TV2A	
	Cat-acc \uparrow	Cnt-acc \uparrow	Ord-acc \uparrow	IS \uparrow	FAD \downarrow	IS \uparrow	FAD \downarrow	IS \uparrow	FAD \downarrow
Labels	17.35	2.80	4.60	7.59	6.02	10.46	1.81	10.62	3.41
AudioSetCaps	27.85	6.40	4.80	10.08	3.19	11.35	1.33	12.39	1.56
QwenCap	24.60	6.40	6.20	9.74	4.40	10.57	1.67	11.79	1.95
GeminiCap	28.05	9.60	7.60	10.81	3.02	11.48	1.31	12.78	1.70
GeminiCap-aug	28.91	10.20	7.80	10.93	2.91	11.69	1.15	12.90	1.48

452
 453
 454 **Table 4: Ablation study of the MAF architecture components.** We evaluate the contribution of
 455 the Gate and Query mechanisms by removing them individually. The results show that the *Full*
 456 *MAF*, which includes both components, achieves the best performance across most metrics. This
 457 confirms that our complete design is essential for effective multimodal fusion.

Components	Gate	Query	KL \downarrow	IS \uparrow	FD \downarrow	FAD \downarrow	Duration \downarrow	Frequency \downarrow	Ordering \downarrow
w/o MAF	\times	\times	1.83	10.70	11.60	2.67	3.022	1.359	0.912
w/o Gate	\times	\checkmark	1.69	11.66	9.72	2.00	2.945	1.348	0.876
w/o Query	\checkmark	\times	1.71	11.72	9.65	2.08	2.841	1.328	0.912
Full MAF	\checkmark	\checkmark	1.68	11.84	9.64	1.98	2.827	1.302	0.888

463
 464 **Architectural ablation of the MAF module.** We conduct an architectural ablation of the MAF
 465 module to validate its design (Table 4). The results confirm that each component is integral, with
 466 the most severe performance deterioration observed when the MAF module is omitted entirely. Re-
 467 moving the Gate mechanism or the Query-based attention individually also results in a performance
 468 decline, confirming their respective contributions. This analysis validates our design choices, un-
 469 der scoring that the complete MAF architecture is critical for optimal multimodal fusion, thereby
 470 enhancing cross-modal alignment and improving generation quality.

471 5.5 DISCUSSION

472 Our extensive experiments provide a multi-faceted validation of *AudioX*, consistently demonstrating
 473 state-of-the-art performance from broad audio generation to a commanding lead in fine-grained
 474 instruction-following. Our ablation studies confirm that this success is directly attributable to two
 475 core principles: a data curation strategy that provides a rich semantic foundation via a powerful
 476 cross-modal regularization effect, and an MAF architecture essential for translating these signals
 477 into precisely controlled outputs. The synergy between this data-centric foundation and purpose-
 478 built architecture culminates in our model’s SOTA performance on challenging instruction-following
 479 benchmarks, validating our approach for unifying generative versatility with fine-grained control.

480 6 CONCLUSION

481
 482 In this work, we present *AudioX*, a unified framework that transcends the modality and domain con-
 483 straints prevalent in prior specialist models for audio generation. By leveraging a DiT backbone and
 484 our designed MAF module, our model effectively unifies diverse inputs like text, video, and audio

486 to produce high-quality outputs. The training of our model is supported by IF-caps, our large-scale,
 487 fine-grained dataset, which provides a robust foundation for unified training and evaluation. Notably,
 488 our training methodology induces an effective cross-modal regularization effect, enhancing the
 489 model’s internal representations. Extensive experiments demonstrate that our single, unified model
 490 not only matches or outperforms specialist models but also unlocks superior instruction-following
 491 capabilities, showcasing its command of both generative versatility and fine-grained control.
 492

493 ETHICS STATEMENT

494
 495 The authors have adhered to the ICLR Code of Ethics. Our work is intended to foster positive and
 496 creative applications in media, and we have carefully considered the ethical implications of our re-
 497 search. The IF-caps dataset is curated exclusively from publicly available sources, and its release
 498 will fully comply with the licenses of the original material. Our human evaluation involved com-
 499 pensated professional experts who provided informed consent. No conflicts of interest or sponsorship
 500 bias exist in this work, and all authors adhere to research integrity practices, including transparent
 501 documentation of data sources, collection procedures, and evaluation protocols. By committing to
 502 open-sourcing our code, model, and dataset, we aim to ensure transparency and support the commu-
 503 nity in the responsible advancement of generative audio technology.
 504

505 REPRODUCIBILITY STATEMENT

506
 507 We are committed to ensuring the reproducibility of our work and have provided comprehensive
 508 details of our methodology and experiments. The complete architecture of our AudioX frame-
 509 work, including the Multimodal Adaptive Fusion module, is detailed in Section 4.1 and visualized
 510 in Figure 4. All implementation details, including optimizer settings, learning rates, batch sizes, and
 511 computational resources, are provided in Section 5.1. Our data curation pipeline for constructing the
 512 IF-caps dataset is described in Section 3, with further details on the annotation schema, data statis-
 513 tics, and augmentation samples available in Appendix A.1.1. Our full evaluation protocol, including
 514 precise definitions for all objective and subjective metrics and the design of our new benchmark,
 515 T2A-bench, is detailed in Section 5.2, Appendix A.2, and Appendix A.3. To further aid replication
 516 and future research, we will open-source our code, pretrained model checkpoints, and the complete
 517 IF-caps dataset upon publication.
 518

519 REFERENCES

520 Jinze Bai, Shuai Bai, Shusheng Yang, Shijie Wang, Sinan Tan, Peng Wang, Junyang Lin, Chang
 521 Zhou, and Jingren Zhou. Qwen-vl: A frontier large vision-language model with versatile abilities.
 522 *arXiv preprint arXiv:2308.12966*, 2023.

523 Jisheng Bai, Haohe Liu, Mou Wang, Dongyuan Shi, Wenwu Wang, Mark D Plumbley, Woon-Seng
 524 Gan, and Jianfeng Chen. Audiosetcaps: An enriched audio-caption dataset using automated gen-
 525 eration pipeline with large audio and language models. *IEEE Transactions on Audio, Speech and*
 526 *Language Processing*, 2025.

527 Tim Brooks, Aleksander Holynski, and Alexei A Efros. Instructpix2pix: Learning to follow image
 528 editing instructions. In *Proceedings of the IEEE/CVF Conference on Computer Vision and Pattern*
 529 *Recognition*, pp. 18392–18402, 2023.

530 Haoxin Chen, Menghan Xia, Yingqing He, Yong Zhang, Xiaodong Cun, Shaoshu Yang, Jinbo Xing,
 531 Yaofang Liu, Qifeng Chen, Xintao Wang, et al. Videocrafter1: Open diffusion models for high-
 532 quality video generation. *arXiv preprint arXiv:2310.19512*, 2023.

533 Honglie Chen, Weidi Xie, Andrea Vedaldi, and Andrew Zisserman. Vggsound: A large-scale audio-
 534 visual dataset. In *ICASSP 2020-2020 IEEE International Conference on Acoustics, Speech and*
 535 *Signal Processing (ICASSP)*, pp. 721–725. IEEE, 2020.

536 Xin Chen. Animeganv2. <https://github.com/TachibanaYoshino/AnimeGANv2/>,
 537 2022.

540 Ziyang Chen, Prem Seetharaman, Bryan Russell, Oriol Nieto, David Bourgin, Andrew Owens, and
 541 Justin Salamon. Video-guided foley sound generation with multimodal controls. *arXiv preprint*
 542 *arXiv:2411.17698*, 2024.

543

544 Ho Kei Cheng, Masato Ishii, Akio Hayakawa, Takashi Shibuya, Alexander Schwing, and Yuki Mit-
 545 sufuji. Mmaudio: Taming multimodal joint training for high-quality video-to-audio synthesis.
 546 In *Proceedings of the Computer Vision and Pattern Recognition Conference*, pp. 28901–28911,
 547 2025.

548 Yunfei Chu, Jin Xu, Qian Yang, Haojie Wei, Xipin Wei, Zhifang Guo, Yichong Leng, Yuanjun Lv,
 549 Jinzheng He, Junyang Lin, et al. Qwen2-audio technical report. *arXiv preprint arXiv:2407.10759*,
 550 2024.

551 Jade Copet, Felix Kreuk, Itai Gat, Tal Remez, David Kant, Gabriel Synnaeve, Yossi Adi, and Alexan-
 552 dre Défossez. Simple and controllable music generation. *Advances in Neural Information Pro-
 553 cessing Systems*, 36, 2024.

554 Shangzhe Di, Zeren Jiang, Si Liu, Zhaokai Wang, Leyan Zhu, Zexin He, Hongming Liu, and
 555 Shuicheng Yan. Video background music generation with controllable music transformer. In
 556 *Proceedings of the 29th ACM International Conference on Multimedia*, pp. 2037–2045, 2021.

557

558 Chris Donahue, Julian McAuley, and Miller Puckette. Adversarial audio synthesis. *arXiv preprint*
 559 *arXiv:1802.04208*, 2018.

560

561 Konstantinos Drossos, Samuel Lipping, and Tuomas Virtanen. Clotho: An audio captioning dataset.
 562 In *ICASSP 2020-2020 IEEE International Conference on Acoustics, Speech and Signal Process-
 563 ing (ICASSP)*, pp. 736–740. IEEE, 2020.

564

565 Benjamin Elizalde, Soham Deshmukh, Mahmoud Al Ismail, and Huaming Wang. Clap learning
 566 audio concepts from natural language supervision. In *ICASSP 2023-2023 IEEE International
 567 Conference on Acoustics, Speech and Signal Processing (ICASSP)*, pp. 1–5. IEEE, 2023.

568

569 Zach Evans, Julian D Parker, CJ Carr, Zack Zukowski, Josiah Taylor, and Jordi Pons. Long-form
 570 music generation with latent diffusion. *arXiv preprint arXiv:2404.10301*, 2024a.

571

572 Zach Evans, Julian D Parker, CJ Carr, Zack Zukowski, Josiah Taylor, and Jordi Pons. Stable audio
 573 open. *arXiv preprint arXiv:2407.14358*, 2024b.

574

575 Jort F Gemmeke, Daniel PW Ellis, Dylan Freedman, Aren Jansen, Wade Lawrence, R Channing
 576 Moore, Manoj Plakal, and Marvin Ritter. Audio set: An ontology and human-labeled dataset for
 577 audio events. In *2017 IEEE international conference on acoustics, speech and signal processing
 578 (ICASSP)*, pp. 776–780. IEEE, 2017.

579

580 Deepanway Ghosal, Navonil Majumder, Ambuj Mehrish, and Soujanya Poria. Text-to-audio gen-
 581 eration using instruction-tuned llm and latent diffusion model. *arXiv preprint arXiv:2304.13731*,
 582 2023.

583

584 Rohit Girdhar, Alaaeldin El-Nouby, Zhuang Liu, Mannat Singh, Kalyan Vasudev Alwala, Armand
 585 Joulin, and Ishan Misra. Imagebind: One embedding space to bind them all. In *Proceedings of
 586 the IEEE/CVF Conference on Computer Vision and Pattern Recognition*, pp. 15180–15190, 2023.

587

588 Yuwei Guo, Ceyuan Yang, Anyi Rao, Zhengyang Liang, Yaohui Wang, Yu Qiao, Maneesh
 589 Agrawala, Dahua Lin, and Bo Dai. Animatediff: Animate your personalized text-to-image diffu-
 590 sion models without specific tuning. *arXiv preprint arXiv:2307.04725*, 2023.

591

592 Yingqing He, Zhaoyang Liu, Jingye Chen, Zeyue Tian, Hongyu Liu, Xiaowei Chi, Runtao Liu,
 593 Ruibin Yuan, Yazhou Xing, Wenhui Wang, et al. Llms meet multimodal generation and editing:
 594 A survey. *arXiv preprint arXiv:2405.19334*, 2024.

595

596 Shawn Hershey, Sourish Chaudhuri, Daniel PW Ellis, Jort F Gemmeke, Aren Jansen, R Channing
 597 Moore, Manoj Plakal, Devin Platt, Rif A Saurous, Bryan Seybold, et al. Cnn architectures for
 598 large-scale audio classification. In *2017 ieee international conference on acoustics, speech and
 599 signal processing (icassp)*, pp. 131–135. IEEE, 2017.

594 Shawn Hershey, Daniel PW Ellis, Eduardo Fonseca, Aren Jansen, Caroline Liu, R Channing Moore,
 595 and Manoj Plakal. The benefit of temporally-strong labels in audio event classification. In
 596 *ICASSP 2021-2021 IEEE International Conference on Acoustics, Speech and Signal Processing*
 597 (*ICASSP*), pp. 366–370. IEEE, 2021.

598 Martin Heusel, Hubert Ramsauer, Thomas Unterthiner, Bernhard Nessler, and Sepp Hochreiter.
 599 Gans trained by a two time-scale update rule converge to a local nash equilibrium. *Advances in*
 600 *neural information processing systems*, 30, 2017.

602 Jonathan Ho, Ajay Jain, and Pieter Abbeel. Denoising diffusion probabilistic models. *Advances in*
 603 *neural information processing systems*, 33:6840–6851, 2020.

604 Jonathan Ho, Tim Salimans, Alexey Gritsenko, William Chan, Mohammad Norouzi, and David J
 605 Fleet. Video diffusion models. *Advances in Neural Information Processing Systems*, 35:8633–
 606 8646, 2022.

608 Jiawei Huang, Yi Ren, Rongjie Huang, Dongchao Yang, Zhenhui Ye, Chen Zhang, Jinglin Liu,
 609 Xiang Yin, Zejun Ma, and Zhou Zhao. Make-an-audio 2: Temporal-enhanced text-to-audio gen-
 610 eration. *arXiv preprint arXiv:2305.18474*, 2023.

611 Vladimir Iashin, Weidi Xie, Esa Rahtu, and Andrew Zisserman. Synchformer: Efficient synchro-
 612 nization from sparse cues. In *ICASSP 2024-2024 IEEE International Conference on Acoustics,*
 613 *Speech and Signal Processing (ICASSP)*, pp. 5325–5329. IEEE, 2024.

615 Myeonghun Jeong, Hyeongju Kim, Sung Jun Cheon, Byoung Jin Choi, and Nam Soo Kim. Diff-tts:
 616 A denoising diffusion model for text-to-speech. *arXiv preprint arXiv:2104.01409*, 2021.

617 Yuxuan Jiang, Zehua Chen, Zeqian Ju, Chang Li, Weibei Dou, and Jun Zhu. Freeaudio:
 618 Training-free timing planning for controllable long-form text-to-audio generation. *arXiv preprint*
 619 *arXiv:2507.08557*, 2025.

621 Jaeyong Kang, Soujanya Poria, and Dorien Herremans. Video2music: Suitable music generation
 622 from videos using an affective multimodal transformer model. *Expert Systems with Applications*,
 623 249:123640, 2024.

625 Chris Dongjoo Kim, Byeongchang Kim, Hyunmin Lee, and Gunhee Kim. Audiocaps: Generating
 626 captions for audios in the wild. In *Proceedings of the 2019 Conference of the North American*
 627 *Chapter of the Association for Computational Linguistics: Human Language Technologies, Vol-*
 628 *ume 1 (Long and Short Papers)*, pp. 119–132, 2019.

629 Qiuqiang Kong, Yin Cao, Turab Iqbal, Yuxuan Wang, Wenwu Wang, and Mark D Plumbley. Panns:
 630 Large-scale pretrained audio neural networks for audio pattern recognition. *IEEE/ACM Transac-*
 631 *tions on Audio, Speech, and Language Processing*, 28:2880–2894, 2020.

633 Felix Kreuk, Gabriel Synnaeve, Adam Polyak, Uriel Singer, Alexandre Défossez, Jade Copet, Devi
 634 Parikh, Yaniv Taigman, and Yossi Adi. Audiogen: Textually guided audio generation. *arXiv*
 635 *preprint arXiv:2209.15352*, 2022.

636 Ruiqi Li, Siqi Zheng, Xize Cheng, Ziang Zhang, Shengpeng Ji, and Zhou Zhao. Muvi: Video-
 637 to-music generation with semantic alignment and rhythmic synchronization. *arXiv preprint*
 638 *arXiv:2410.12957*, 2024a.

639 Sizhe Li, Yiming Qin, Minghang Zheng, Xin Jin, and Yang Liu. Diff-bgm: A diffusion model for
 640 video background music generation. In *Proceedings of the IEEE/CVF Conference on Computer*
 641 *Vision and Pattern Recognition*, pp. 27348–27357, 2024b.

643 Bin Lin, Yang Ye, Bin Zhu, Jiaxi Cui, Munan Ning, Peng Jin, and Li Yuan. Video-llava: Learning
 644 united visual representation by alignment before projection. *arXiv preprint arXiv:2311.10122*,
 645 2023.

646 Yan-Bo Lin, Yu Tian, Linjie Yang, Gedas Bertasius, and Heng Wang. Vmas: Video-to-music gen-
 647 eration via semantic alignment in web music videos. *arXiv preprint arXiv:2409.07450*, 2024.

648 Haohe Liu, Zehua Chen, Yi Yuan, Xinhao Mei, Xubo Liu, Danilo Mandic, Wenwu Wang, and
 649 Mark D Plumbley. Audioldm: Text-to-audio generation with latent diffusion models. *arXiv*
 650 *preprint arXiv:2301.12503*, 2023.

651

652 Haohe Liu, Yi Yuan, Xubo Liu, Xinhao Mei, Qiuqiang Kong, Qiao Tian, Yuping Wang, Wenwu
 653 Wang, Yuxuan Wang, and Mark D Plumbley. Audioldm 2: Learning holistic audio generation
 654 with self-supervised pretraining. *IEEE/ACM Transactions on Audio, Speech, and Language Pro-*
 655 *cessing*, 2024a.

656 Haotian Liu, Chunyuan Li, Qingyang Wu, and Yong Jae Lee. Visual instruction tuning. *Advances*
 657 *in neural information processing systems*, 36, 2024b.

658

659 Jinglin Liu, Chengxi Li, Yi Ren, Feiyang Chen, and Zhou Zhao. Diffssinger: Singing voice synthesis
 660 via shallow diffusion mechanism. In *Proceedings of the AAAI conference on artificial intelligence*,
 661 volume 36, pp. 11020–11028, 2022.

662 Shansong Liu, Atin Sakkeer Hussain, Qilong Wu, Chenshuo Sun, and Ying Shan. Mumu-llama:
 663 Multi-modal music understanding and generation via large language models. *arXiv preprint*
 664 *arXiv:2412.06660*, 2024c.

665

666 Simian Luo, Chuanhao Yan, Chenxu Hu, and Hang Zhao. Diff-foley: Synchronized video-to-audio
 667 synthesis with latent diffusion models. *Advances in Neural Information Processing Systems*, 36,
 668 2024.

669

670 Navonil Majumder, Chia-Yu Hung, Deepanway Ghosal, Wei-Ning Hsu, Rada Mihalcea, and Sou-
 671 janya Poria. Tango 2: Aligning diffusion-based text-to-audio generations through direct prefer-
 672 ence optimization. In *Proceedings of the 32nd ACM International Conference on Multimedia*, pp.
 673 564–572, 2024.

674

675 Xinhao Mei, Chutong Meng, Haohe Liu, Qiuqiang Kong, Tom Ko, Chengqi Zhao, Mark D Plumb-
 676 ley, Yuexian Zou, and Wenwu Wang. Wavcaps: A chatgpt-assisted weakly-labelled audio caption-
 677 ing dataset for audio-language multimodal research. *IEEE/ACM Transactions on Audio, Speech,*
 678 *and Language Processing*, 2024.

679

680 Adam Polyak, Amit Zohar, Andrew Brown, Andros Tjandra, Animesh Sinha, Ann Lee, Apoorv
 681 Vyas, Bowen Shi, Chih-Yao Ma, Ching-Yao Chuang, et al. Movie gen: A cast of media founda-
 682 tion models. *arXiv preprint arXiv:2410.13720*, 2024.

683

684 Vadim Popov, Ivan Vovk, Vladimir Gogoryan, Tasnima Sadekova, and Mikhail Kudinov. Grad-
 685 tts: A diffusion probabilistic model for text-to-speech. In *International Conference on Machine*
 686 *Learning*, pp. 8599–8608. PMLR, 2021.

687

688 Alec Radford, Jong Wook Kim, Chris Hallacy, Aditya Ramesh, Gabriel Goh, Sandhini Agarwal,
 689 Girish Sastry, Amanda Askell, Pamela Mishkin, Jack Clark, et al. Learning transferable visual
 690 models from natural language supervision. In *International conference on machine learning*, pp.
 691 8748–8763. PMLR, 2021.

692

693 Colin Raffel, Noam Shazeer, Adam Roberts, Katherine Lee, Sharan Narang, Michael Matena, Yanqi
 694 Zhou, Wei Li, and Peter J Liu. Exploring the limits of transfer learning with a unified text-to-text
 695 transformer. *Journal of machine learning research*, 21(140):1–67, 2020.

696

697 Aditya Ramesh, Prafulla Dhariwal, Alex Nichol, Casey Chu, and Mark Chen. Hierarchical text-
 698 conditional image generation with clip latents. *arXiv preprint arXiv:2204.06125*, 1(2):3, 2022.

699

700 António Ramires, Frederic Font, Dmitry Bogdanov, Jordan BL Smith, Yi-Hsuan Yang, Joann Ching,
 701 Bo-Yu Chen, Yueh-Kao Wu, Hsu Wei-Han, and Xavier Serra. The freesound loop dataset and
 702 annotation tool. *arXiv preprint arXiv:2008.11507*, 2020.

703

704 Robin Rombach, Andreas Blattmann, Dominik Lorenz, Patrick Esser, and Björn Ommer. High-
 705 resolution image synthesis with latent diffusion models. In *Proceedings of the IEEE/CVF confer-
 706 ence on computer vision and pattern recognition*, pp. 10684–10695, 2022.

702 Roy Sheffer and Yossi Adi. I hear your true colors: Image guided audio generation. In *ICASSP 2023-2023 IEEE International Conference on Acoustics, Speech and Signal Processing (ICASSP)*, pp. 703 1–5. IEEE, 2023.

704

705 Yang Song, Jascha Sohl-Dickstein, Diederik P Kingma, Abhishek Kumar, Stefano Ermon, and Ben 706 Poole. Score-based generative modeling through stochastic differential equations. *arXiv preprint 707 arXiv:2011.13456*, 2020.

708

709 Yapeng Tian, Dingzeyu Li, and Chenliang Xu. Unified multisensory perception: Weakly-supervised 710 audio-visual video parsing. In *Computer Vision–ECCV 2020: 16th European Conference, Glasgow, UK, August 23–28, 2020, Proceedings, Part III 16*, pp. 436–454. Springer, 2020.

711

712 Zeyue Tian, Zhaoyang Liu, Ruibin Yuan, Jiahao Pan, Qifeng Liu, Xu Tan, Qifeng Chen, Wei Xue, 713 and Yike Guo. Vidmuse: A simple video-to-music generation framework with long-short-term 714 modeling. In *Proceedings of the Computer Vision and Pattern Recognition Conference*, pp. 715 18782–18793, 2025.

716

717 Andros Tjandra, Yi-Chiao Wu, Baishan Guo, John Hoffman, Brian Ellis, Apoorv Vyas, Bowen 718 Shi, Sanyuan Chen, Matt Le, Nick Zacharov, et al. Meta audiobox aesthetics: Unified automatic 719 quality assessment for speech, music, and sound. *arXiv preprint arXiv:2502.05139*, 2025.

720

721 Yongqi Wang, Wenxiang Guo, Rongjie Huang, Jiawei Huang, Zehan Wang, Fuming You, Ruiqi Li, 722 and Zhou Zhao. Frieren: Efficient video-to-audio generation with rectified flow matching. *arXiv 723 preprint arXiv:2406.00320*, 2024.

724

725 Shengqiong Wu, Hao Fei, Leigang Qu, Wei Ji, and Tat-Seng Chua. Next-gpt: Any-to-any multi- 726 modal llm. *arXiv preprint arXiv:2309.05519*, 2023a.

727

728 Yusong Wu, Ke Chen, Tianyu Zhang, Yuchen Hui, Taylor Berg-Kirkpatrick, and Shlomo Dubnov. 729 Large-scale contrastive language-audio pretraining with feature fusion and keyword-to-caption 730 augmentation. In *ICASSP 2023-2023 IEEE International Conference on Acoustics, Speech and 731 Signal Processing (ICASSP)*, pp. 1–5. IEEE, 2023b.

732

733 Zeyu Xie, Xuenan Xu, Zhizheng Wu, and Mengyue Wu. Audiotime: A temporally-aligned audio- 734 text benchmark dataset. In *ICASSP 2025-2025 IEEE International Conference on Acoustics, 735 Speech and Signal Processing (ICASSP)*, pp. 1–5. IEEE, 2025.

736

737 Yazhou Xing, Yingqing He, Zeyue Tian, Xintao Wang, and Qifeng Chen. Seeing and hearing: Open- 738 domain visual-audio generation with diffusion latent aligners. In *Proceedings of the IEEE/CVF 739 Conference on Computer Vision and Pattern Recognition*, pp. 7151–7161, 2024.

740

741 Yiming Zhang, Yicheng Gu, Yanhong Zeng, Zheneng Xing, Yuancheng Wang, Zhizheng Wu, and 742 Kai Chen. Foleycrafta: Bring silent videos to life with lifelike and synchronized sounds. *arXiv 743 preprint arXiv:2407.01494*, 2024.

744

745 Zitang Zhou, Ke Mei, Yu Lu, Tianyi Wang, and Fengyun Rao. Harmonyset: A comprehensive 746 dataset for understanding video-music semantic alignment and temporal synchronization. In *Pro- 747 ceedings of the Computer Vision and Pattern Recognition Conference*, pp. 3152–3162, 2025.

748

749 Alon Ziv, Itai Gat, Gaël Le Lan, Tal Remez, Felix Kreuk, Jade Copet, Alexandre Défossez, Gabriel 750 Synnaeve, and Yossi Adi. Masked audio generation using a single non-autoregressive transformer. 751 In *The Twelfth International Conference on Learning Representations, ICLR 2024, Vienna, Austria, May 7-11, 2024*. OpenReview.net, 2024a. URL <https://openreview.net/forum?id=Ny8NiVfi95>.

752

753 Alon Ziv, Itai Gat, Gael Le Lan, Tal Remez, Felix Kreuk, Alexandre Défossez, Jade Copet, Gabriel 754 Synnaeve, and Yossi Adi. Masked audio generation using a single non-autoregressive transformer. 755 *arXiv preprint arXiv:2401.04577*, 2024b.

756 **A APPENDIX**
757758 **USE OF LARGE LANGUAGE MODELS**
759760 Large Language Models (LLMs) are utilized in two parts in this work. As components of our
761 methodology, Gemini 2.5 Pro is employed for high-quality initial data annotation, benchmark gen-
762 eration, and as an automated evaluator, while Qwen2-Audio performs large-scale data augmentation.
763 Additionally, an LLM assistant (Google’s Gemini) is used as a writing tool to improve the clarity,
764 grammar, and vocabulary of the manuscript. All scientific ideation, experimental design, and analy-
765 sis are conceived and performed exclusively by the human authors.766 **APPENDIX OVERVIEW**
767769 This appendix supplements the main paper with expanded details on our datasets, evaluation
770 methodologies, and a broader range of experimental results. We begin by detailing our data and
771 evaluation frameworks: Section A.1 delves into the specifics of our datasets and the annotation
772 process, Section A.2 introduces evaluation metrics, while Section A.3 introduces T2A-bench, our
773 benchmark for instruction-following, along with its automated evaluation pipeline. Subsequently,
774 we present an expanded set of results. Section A.4 provides further quantitative comparisons, and
775 finally, Section A.5 showcases a comprehensive gallery of qualitative examples and analyses.776 **A.1 DATASETS**
777778 **A.1.1 TRAINING AND TEST DATASETS**
779780 Table A.1 provides an overview of all datasets used in this work. Table A.2 outlines the new captions
781 we annotated for training and testing our unified model. We will open-source these caption datasets
782 to facilitate further research.783 **A.1.2 FURTHER DETAILS ON THE IF-CAPS DATASET**
784785 As described in the main text, the IF-caps dataset is generated via a multi-step pipeline designed to
786 produce rich, structured annotations for existing video-audio clips. This section provides a detailed
787 breakdown of our annotation schema and showcases representative samples.788 **Annotation Schema.** Each sample in IF-caps is accompanied by a comprehensive set of annotations
789 designed to provide multi-faceted supervision for training. The key fields are as follows:790

- **caption:** A holistic, high-level natural language description of the audio content, summa-
791 rizing the main events and their context.
- **category:** A structured dictionary that provides sound event classification and, where ap-
792 plicable, the discrete count of each event. For continuous or unquantifiable sounds (e.g.,
793 background noise, speech), the count is marked as null.
- **SED (Sound Event Detection):** A list providing fine-grained temporal localization. Each
794 entry in the list maps a precise timestamp (e.g., “00:02-00:06”) to a description of the sound
795 event occurring within that specific time frame.
- **time_relation:** A field describing the temporal relationship between distinct sound events.
796 This can specify a sequential order (e.g., “Event A, Event B”) or more complex relation-
797 ships like “interleave” for overlapping sounds.

804 This structured format allows our model to learn not just what sounds are present, but also how
805 many, when, and in what order, which is critical for developing advanced instruction-following
806 capabilities.807 **Annotation Samples.** Below are two examples from IF-caps that illustrate the richness and de-
808 tail of our annotation schema. The first example demonstrates a complex scene with overlapping,
809 continuous, and countable events. The second example shows a clear sequence of discrete events.

810
 811 Table A.1: Comprehensive overview of training and test datasets, detailing the number of clips (#
 812 Clips), average duration per clip (Dur./Clip in seconds), and total duration (Dur. in hours) for each
 813 task and split. T2A: Text-to-Audio, V2A: Video-to-Audio, TV2A: Text-and-Video-to-Audio, T2M:
 814 Text-to-Music, V2M: Video-to-Music, TV2M: Text-and-Video-to-Music.

815	Split	Task	Dataset	# Clips	Dur./Clip (s)	Dur. (h)
816	Train	T2A	AudioCaps	45.0K	10	125.1
817			WavCaps	108.3K	10	300.8
818			IF-caps	1.3M	10	3524.4
819			AudioTime	20.0K	10	355.5
820		V2A	VGGSound	176.9K	10	491.4
821			AudioSet Strong	67.3K	10	187.1
822			Greatest Hits	1.0K	10	2.7
823		TV2A	IF-caps	1.3M	10	3.5K
824			Greatest Hits	1.0K	10	2.7
825		T2M	Private	175.2K	240	11.7K
826			IF-caps	5.7M	10	15.8K
827			MUCaps	22.0K	208	1.3K
828		V2M	V2M	5.7M	10	15.8K
829			TV2M	5.7M	10	15.8K
830		Audio Inpainting	All audio data	398.5K	10	1.1K
831		Music Completion	All music data	5.9M	17.6	28.8K
832	Test	T2A	AudioCaps	4.9K	10	13.5
833			VGGSound	14.9K	10	41.5
834			T2A-bench	2.0K	10	5.6
835			AudioTime	2.0K	10	5.6
836		V2A	VGGSound	14.9K	10	41.5
837			AVVP	1.1K	10	3.1
838		TV2A	VGGSound	14.9K	10	41.5
839		T2M	MusicCaps	5.5K	10	15.4
840			V2M	3.1K	10	9.0
841		V2M	V2M	300	108	9.0
842			TV2M	300	108	9.0
843		Audio Inpainting	AudioCaps	4.9K	10	13.5
844			AVVP	1.1K	10	3.1
845		Music Completion	V2M	300	108	9.0

846
 847 Table A.2: Overview of our labeled captions, detailing the number of clips, average duration per
 848 clip, and total duration for each source dataset.

849	Source Dataset	Data Type	# Clips	Dur./Clip (s)	Dur. (h)
850	VGGSound	Audio	191.8K	10	532.81
851	AudioSet Strong	Audio	67.3K	10	187.14
852	AVVP Test Split	Audio	1.1K	10	3.11
853	Greatest Hits	Audio	1.0K	10	2.71
854	V2M	Music	5.7M	10	15793.58
855					

856
 857 Example 1:

```

 858 {
 859   "caption": "A woman is speaking continuously, while a dog yips
 860   twice in the background.",
 861   "category": {
 862     "label": "woman speaking"
 863   }
 864 }
```

```

864
865         "Female speech": null,
866         "Yip": 2,
867         "Background noise": null
868     },
869     "SED": [
870         {"00:00-00:09": "A woman is speaking throughout the audio,
871         accompanied by faint background noise."},
872         {"00:00-00:01": "A dog lets out a yip in the background."},
873         {"00:08-00:09": "A dog yips again in the background."}
874     ],
875     "time_relation": "interleave",
876     "audio_id": "TATdZPmzMU8_90000"
877 }

```

877 Example 2:

```

878
879
880     {
881         "caption": "The audio features the mechanical sound of a firearm
882             being handled, immediately followed by two separate bursts of
883             machine gun fire.",
884         "category": {
885             "Machine gun": 2,
886             "Generic impact sounds": 1
887         },
888         "SED": [
889             {"00:00-00:01": "The mechanical sound of a firearm being
890                 handled, possibly being cocked or loaded."},
891             {"00:01-00:05": "A sustained burst of automatic gunfire from
892                 a machine gun."},
893             {"00:06-00:08": "A second, shorter burst of machine gun fire
894                 ."}
895         ],
896         "time_relation": "Generic impact sounds, Machine gun",
897         "audio_id": "c9OnubhhvZY_0"
898     }

```

899 **Data Augmentation Process.** As mentioned in the main text, a key step in our pipeline is to leverage
900 a cost-effective model (Qwen2-Audio) to augment the initial, high-quality annotations generated by
901 Gemini 2.5 Pro. The goal is to increase the linguistic and structural diversity of our dataset. By
902 generating multiple, semantically equivalent but stylistically different captions for the same audio
903 clip, we train our model to be robust to variations in user prompts and to develop a more generalized
904 understanding of the relationship between language and sound. The augmentation process is guided
905 by the structured fields of the original annotation. The model is prompted to generate new cap-
906 tions from different perspectives: rephrasing the original description, or generating new descriptions
907 based purely on the category and count, the SED timestamps, or the time_relation fields. Below, we
908 use the second example from the previous section to illustrate this structured augmentation process.

909 Original Audio Annotation (Generated by Gemini 2.5 Pro)

```

910
911     {
912         "caption": "The audio features the mechanical sound of a firearm
913             being handled, immediately followed by two separate bursts of
914             machine gun fire.", "category": {"Machine gun": 2, "Generic
915             impact sounds": 1}, "SED": [...], "time_relation": "Generic
916             impact sounds, Machine gun", "audio_id": "c9OnubhhvZY_0"}
917

```

918 This single, rich annotation serves as the seed for generating a variety of new training captions, each
919 emphasizing a different aspect of the audio content.

920

918
919

Augmented Audio Captions (Generated by Qwen2-Audio)

920

1. Caption Rephrasing (Linguistic Diversity)

921

“A gun is cocked, followed by two bursts of machine gun fire.”

922

“After the sharp, metallic sound of a firearm mechanism, two rapid-fire bursts from a machine gun are heard.”

923

2. Augmentation from Category and Count

924

925

“The audio contains two sounds of a machine gun and one generic impact sound.”

926

927

3. Augmentation from SED

928

929

930

931

“The sound of a firearm being handled is audible for the first second, followed by a burst of machine gun fire from 1 to 5 seconds and a second burst from 6 to 8 seconds.”

932

4. Augmentation from Time Relation

933

934

935

“In this audio, the sound of a generic impact occurs first, followed by two distinct machine gun sounds.”

This structured augmentation strategy ensures our model is exposed to a wide variety of textual descriptions, learning to associate not only high-level captions but also explicit instructions about count, timing, and order with the corresponding audio features. Similarly, for music data, this process generates varied descriptions of genre, mood, instrumentation, and tempo, teaching the model to comprehend both high-level artistic direction and specific musical components.

936

Original Music Annotation (Generated by Gemini 2.5 Pro)

937

938

939

940

941

942

943

944

945

946

947

948

949

```
{"caption": "A heartwarming acoustic track featuring a blend of
softly strummed guitar and a simple, melodic piano line,
creating a gentle and uplifting atmosphere.", "genre": "Acoustic
Pop, Instrumental", "mood": "Heartwarming, Gentle, Uplifting",
"instrument": ["Acoustic Guitar", "Piano"], "tempo": "Slow to
Moderate"}
```

This structured music annotation is then used to generate diverse new training captions, each focusing on a different attribute:

950

951

Augmented Music Captions (Generated by Qwen2-Audio)

952

953

1. Caption Rephrasing

954

955

956

957

958

959

960

961

962

963

964

965

966

967

968

969

970

971

*“A gentle instrumental piece with the interwoven sounds of an acoustic guitar and piano.”**“Soft guitar strumming and a simple piano melody combine to create an uplifting acoustic pop track.”***2. Augmentation from Genre***“An instrumental acoustic pop track featuring piano and guitar.”***3. Augmentation from Mood***“A heartwarming, gentle, and uplifting piece of music featuring acoustic guitar and piano.”***4. Augmentation from Tempo***“A slow to moderate tempo instrumental track with piano and acoustic guitar.”*

972

A.2 DETAILS OF EVALUATION METRICS

973

974

975

Fréchet Audio Distance (FAD). To evaluate the perceptual quality of the generated audio, we employ FAD, a reference-free metric analogous to the FID (Heusel et al., 2017) score used in image generation. The metric functions by comparing the statistical distance between embedding distributions of generated audio and real-world audio. A smaller distance suggests the generated audio is of higher acoustic quality. For our calculations, we utilize the VGGish (Hershey et al., 2017) feature extractor.

981

Fréchet Distance (FD). While similar in principle to FAD, FD serves as a distinct measure of audio similarity by employing a different feature extractor. We use an FD variant based on PANNs (Kong et al., 2020) embeddings. Given that PANNs models are pretrained on the extensive AudioSet (Gemmeke et al., 2017), this metric is considered to be highly robust for evaluating audio fidelity.

985

Kullback-Leibler Divergence (KL). The KL divergence is used to approximate the acoustic similarity between generated and reference audio samples. This is achieved by measuring the divergence between the multi-label class prediction distributions produced by a PANNs model for both sets of samples.

989

Inception Score (IS). The IS is a widely used metric to evaluate the performance of generative models. Besides assessing the diversity of the generated samples, IS also evaluates their quality, measuring the clarity and recognizability of individual audio events (Donahue et al., 2018; Majumder et al., 2024; Liu et al., 2023). Given its ability to provide a single, holistic score reflecting both of these aspects without needing a reference prompt, we selected IS as the unified metric for the comprehensive performance comparison in our teaser Fig. 1. This allows for a fair and consistent visualization of our model’s capabilities across the wide array of supported tasks.

996

ImageBind Score (Girdhar et al., 2023). We assess the semantic alignment between generated audio and conditioning videos using the ImageBind Score. This score is calculated as the cosine similarity between the audio and video embeddings from the respective branches of the ImageBind model.

1000

CLAP Score. The Contrastive Language-Audio Pretraining (CLAP) model (Elizalde et al., 2023) learns a joint embedding space where audio clips and their corresponding text descriptions are aligned. We use the CLAP Score to evaluate the semantic alignment between generated audio and a text prompt, calculated as the cosine similarity between their respective embeddings from the pretrained CLAP encoders (Wu et al., 2023b). A higher score indicates better alignment.

1005

Production Complexity (PC) and Production Quality (PQ). These metrics are derived from the Meta Audiobox Aesthetics framework (Tjandra et al., 2025). PQ focuses on the objective, technical aspects of an audio recording, such as its clarity, fidelity, dynamics, and frequency balance. In contrast, PC evaluates the complexity of an audio scene by measuring the number of distinct audio components present, such as multiple instruments or the co-occurrence of speech, music, and sound effects. Both are designed as no-reference metrics, allowing for the assessment of individual audio clips without needing a ground-truth comparison sample.

1012

Ordering, Duration, Frequency, and Timestamp. These metrics are components of the STEAM evaluation framework, proposed in the AudioTime (Xie et al., 2025) to assess the temporal controllability of audio generation models. Ordering is an error rate that measures whether sound events are generated in the specified sequence. Duration and Frequency are calculated as the L1 error between the specified and detected event durations and occurrence counts, respectively. Timestamp evaluates the precise timing of events (onset and offset) using the F1-score, a common metric in sound event detection.

1019

Category, Count, Ordering, and Timestamp accuracy. See A.3.

1021

Overall Quality (OVL) and Relevance (REL). For our subjective evaluation, 10 professional audio experts rated each generated sample on a scale of 1 to 100 on two standard criteria. OVL assesses the intrinsic perceptual fidelity of the audio itself—focusing on aspects like clarity and freedom from artifacts—*independent* of the prompt. In parallel, REL measures the semantic alignment between the audio and its conditioning input, evaluating how accurately the content reflects the instructions from the provided text or video. This evaluation protocol follows the established methodologies of

1026 prior work (Kreuk et al., 2022; Liu et al., 2023). Example of the questionnaire interface is shown in
 1027 Table A.3.

1029
 1030 Table A.3: Simplified example of the questionnaire for human evaluation, showcasing the four main
 1031 task types. Experts provided scores for OVL and REL.

File Name	Prompt (Text or Video)	OVL (1-100)	REL (1-100)
9964.wav	A loud white noise and then some beeping.	55	65
0928.wav	An uplifting folk-pop instrumental track.	70	55
1441.wav	[Video of a person walking on dry leaves]	80	70
1701.wav	[Video of a drone shot over a sunrise mountain]	65	60
...

1040 A.3 BENCHMARK AND METRICS FOR INSTRUCTION-FOLLOWING IN T2A

1042 To rigorously and scalably evaluate the instruction-following capabilities of Text-to-Audio genera-
 1043 tion models, we introduce a new benchmark, **T2A-bench**, and a corresponding automated evaluation
 1044 pipeline. This framework is designed to dissect a model’s ability to adhere to complex compositional
 1045 instructions.



1057 Figure A.1: The composition of the T2A-bench benchmark. (a) Word cloud of sound event cate-
 1058 gories. (b) Distribution of task types and category counts.

1060 **T2A-bench Composition and Design.** T2A-bench is a prompt-based benchmark comprising 2k
 1061 challenging, natural language prompts generated by Gemini 2.5 Pro. It is structured to systemat-
 1062 ically probe four key dimensions of controllability. As illustrated in Figure A.1, our benchmark
 1063 encompasses a diverse vocabulary of sound categories and a balanced task structure to enable a rig-
 1064 orous and comprehensive evaluation. The benchmark is divided into four task types, each containing
 1065 500 prompts:

- 1067 • **Category-only:** Evaluates the generation of correct sound events. Prompts contain be-
 1068 tween one and five distinct sound categories (100 prompts for each count).
- 1069 • **Category+Count:** Assesses the ability to generate a precise number of sound events. To
 1070 avoid ambiguity, prompts in this category feature only a single sound type, with the required
 1071 count ranging from one to five (100 prompts for each count).
- 1073 • **Category+Ordering:** Measures adherence to temporal sequence. Prompts specify an order
 1074 for either two or three distinct sound categories.
- 1076 • **Category+Timestamp:** Tests temporal localization. To ensure clarity, prompts specify a
 1077 start and end time for a single sound category.

1078 Below are representative examples for each task type, including the prompt and its corresponding
 1079 structured metadata.

```

1080 T2A-bench Examples
1081
1082
1083 {
1084     "id": "T2A_01565",
1085     "type": "category-only",
1086     "prompt": "A violent storm at sea, with a loud clap of thunder and a
1087         huge wave crashing over the deck.",
1088     "category": "thunder, wave crash"
1089 }
1090 {
1091     "id": "T2A_00031",
1092     "type": "category+count",
1093     "prompt": "A single, loud bark from a dog in the distance.",
1094     "category": "dog bark",
1095     "count": {"dog bark": 1}
1096 }
1097 {
1098     "id": "T2A_00575",
1099     "type": "category+ordering",
1100     "prompt": "The sound of a person gargling, followed by the splash of
1101         water in the sink.",
1102     "category": "gargle, water splash",
1103     "time_relation": "gargle, water splash"
1104 }
1105 {
1106     "id": "T2A_01105",
1107     "type": "category+timestamp",
1108     "prompt": "The sound of a crowd cheering is present from 2.0 seconds
1109         to 6.0 seconds.",
1110     "category": "crowd cheering",
1111     "timestamp": {"crowd cheering": {"start": 2.0, "end": 6.0}}
1112 }
```

1109 **Evaluation Metrics.** Corresponding to the benchmark’s structure, we define four strict, accuracy-
1110 based metrics: Category Accuracy (Cat-acc), Count Accuracy (Cnt-acc), Ordering Accuracy (Ord-
1111 acc), and Timestamp Accuracy (TS-acc). The final score for each metric is the percentage of “cor-
1112 rect” judgments.

1113

- 1114 • **Cat-acc:** A judgment is “correct” only if *all* sound categories specified in the prompt are
1115 detected in the generated audio. This is evaluated on all 2,000 samples.
- 1116 • **Cnt-acc:** A judgment is “correct” only if the detected count for the specified category
1117 exactly matches the prompt’s instruction.
- 1118 • **Ord-acc:** A judgment is “correct” only if the detected temporal order of sound events
1119 exactly matches the specified sequence.
- 1120 • **TS-acc:** A judgment is “correct” only if the detected event’s start and end times fall within
1121 a 1-second tolerance window of the target times specified in the prompt.

1123 **Automated Evaluation Pipeline.** To ensure objective and scalable evaluation while preventing
1124 information leakage, we designed a novel two-step pipeline that leverages the state-of-the-art audio
1125 understanding of a powerful Multimodal Large Model (MLLM), Gemini 2.5 Pro, as an automated
1126 judge.

1128

- 1129 • **Step 1: Blind Audio Annotation.** In the first step, the MLLM judge receives *only* the audio
1130 sample generated by the model under evaluation. It performs a blind, detailed analysis to
1131 produce a structured annotation of the audio’s content. This annotation includes detected
1132 sound categories, their counts, temporal relationships, and precise sound event detection
1133 (SED) timestamps. For sounds where counting is ambiguous (e.g., continuous water flow)
or ordering is not distinct, the corresponding fields are populated with null.

1134
1135
1136
1137
1138
1139
1140
1141
1142
1143
1144
1145
1146
1147

```
Example of Step 1 Output (Structured Annotation)

{
  "caption": "The audio contains two distinct loud sounds.
    First, there is a deep, rolling thunderclap. After a
    brief pause, a powerful and sudden explosion is heard.",
  "category": {"Thunder": 1, "Explosion": 1},
  "SED": [
    {"00:01.734-00:03.514": "A deep, rolling thunderclap
      is heard."},
    {"00:08.241-00:09.511": "A loud and sudden explosion
      with a distinct boom."}],
  "time_relation": "Thunder, Explosion",
}
```

1148
1149
1150
1151
1152
1153

- **Step 2: LLM-based Judgment.** In the second step, the MLLM judge is provided with the original prompt from T2A-bench and the structured annotation generated in Step 1. Acting like an examiner with an answer key, the MLLM compares the annotated audio content against the prompt’s instructions. It then outputs a binary score (1 for correct, 0 for incorrect) for the relevant metric, along with a detailed textual analysis explaining its decision.

1154
1155
1156
1157
1158
1159
1160
1161
1162
1163
1164
1165
1166
1167
1168

```
Example of Step 2 Output (Final Judgment)

{
  "prompt": "A medieval battlefield, with the sound of a
    catapult launching a stone and the subsequent explosion."
  "prediction": {"cat_acc": 0, "cnt_acc": null, "ord_acc": null
    , "ts_acc": null,
  "analysis": "The audio contains a clear and prominent sound
    of thunder, which is audible from the beginning and
    culminates in a loud clap around 00:03. However, the
    required category 'wave crash' is missing. While there is
    a sound of water starting around 00:05, it is
    acoustically identifiable as heavy rain rather than a
    distinct, powerful wave crashing."}
}
```

1169
1170
1171
1172

In summary, our framework, combining T2A-bench, fine-grained metrics, and a robust two-step evaluation pipeline, provides a comprehensive and replicable methodology for quantifying the instruction-following capabilities of T2A models. We will open-source our proposed benchmark and evaluation pipeline to facilitate future research in this area.

1173

A.4 MORE RESULTS

1174
1175
1176

A.4.1 COMPARISON RESULTS

1177
1178
1179
1180
1181
1182
1183
1184

Audio inpainting. As shown in Table A.4, we conducted experiments on audio inpainting tasks, where our model outperformed the baselines (Liu et al., 2023; 2024a) on the AudioCaps (Kim et al., 2019) and AVVP (Tian et al., 2020) test datasets. Additionally, to explore audio inpainting with various input modalities, we performed experiments on unconditioned audio inpainting, as well as video-guided and text-and-video-guided audio inpainting tasks (on AVVP). The results indicate that both text and video can effectively guide the audio inpainting task, with text providing better guidance than video. When both text and video are conditioned, the model can integrate the two modalities to achieve superior results.

1185
1186
1187

Music Completion. Music completion is a task where the model generates music based on a given music clip. We evaluate our model on the V2M-bench (Tian et al., 2025) dataset. The results are shown in Table A.5. We find that our model can generate music that extends the input music clip. As the number of input modalities increases, the model’s performance improves, demonstrating its

1188
 1189 **Table A.4: Inpainting Performance Comparison.** This table shows the performance comparison
 1190 for audio inpainting on the AudioCaps and AVVP datasets. The values before and after the slash
 1191 represent the IS and FAD metrics, respectively. A, V, and T represent Audio, Video, and Text
 1192 conditions. The baseline methods are all under audio and text conditions.

Method	Input	Dataset	
		AudioCaps	AVVP
Unprocessed	-	6.51/11.34	4.94/6.70
AudioLDM-L-Full(Liu et al., 2024a)	A+T	8.06/2.64	5.11/3.30
AudioLDM-2-Full-Large(Liu et al., 2024a)	A+T	4.24/10.17	3.99/11.58
AudioX	A	4.63/5.35	3.94/5.44
AudioX	A+T	9.84/2.25	<u>6.12/2.05</u>
AudioX	A+V	N/A	5.63/2.16
AudioX	A+T+V	N/A	6.25/1.99

1201
 1202 strong inter-modal learning capability and ability to leverage multi-modal information to generate
 1203 better music.

1204
 1205
 1206 **Table A.5: Performance for our method under different conditions in the music completion**
 1207 **task.** M, T, and V represent Music, Text, and Video, respectively.

Input	KL ↓	IS ↑	FD ↓	FAD ↓
M	0.96	1.21	52.77	5.76
T+M	<u>0.51</u>	<u>1.49</u>	<u>21.42</u>	<u>2.14</u>
V+M	0.70	1.37	24.28	2.29
T+V+M	0.46	1.52	18.69	1.67

1214
 1215 **Image-to-audio generation.** To evaluate the model’s capability in handling static visual inputs, we
 1216 conduct a **zero-shot image-to-audio generation** experiment. Adopting the experimental protocol
 1217 of Seeing&Hearing (Xing et al., 2024), we perform evaluations on 3k clips from the VGGSound test
 1218 set, where keyframes were processed using AnimeGANv2 (Chen, 2022) to transfer them into “Pa-
 1219 prika style” prior to generation. For comparison, we benchmark AudioX against Seeing&Hearing
 1220 (Xing et al., 2024), Im2Wav (Sheffer & Adi, 2023), and also constructed a baseline by combining
 1221 an image caption model (Bai et al., 2023) with a text-to-audio model (Majumder et al., 2024). The
 1222 results are shown in Table A.6 in the Appendix. We find that our model demonstrates excellent
 1223 performance in the image-to-audio generation task even without any specific training with image
 1224 data.

1225
 1226 **Table A.6: Comparison of Methods for the Image2Audio Task.**

Method	KL ↓	IS ↑	FD ↓	FAD ↓	Align. ↑
Caption2Audio	2.76	<u>7.48</u>	32.97	<u>5.54</u>	0.21
Im2Wav(Sheffer & Adi, 2023)	2.61	<u>7.06</u>	<u>19.63</u>	7.58	0.41
Seeing&Hearing(Xing et al., 2024)	2.69	6.15	20.96	6.87	<u>0.29</u>
AudioX	2.90	13.48	16.42	2.71	0.23

1232
 1233 **User study.** We conducted a user study to evaluate the quality of the generated audio and music. We
 1234 randomly selected 25 samples for each audio generation task, including text-to-audio (T2A), text-
 1235 to-music (T2M), video-to-audio (V2A), and video-to-music (V2M). 10 audio experts are asked to
 1236 rate the quality of the generated audio and music. The results are shown in Fig. A.2. The evaluation
 1237 shows that our model achieves subjective SOTA performance in terms of OVL and REL scores in
 1238 most tasks, indicating high user satisfaction.

1239
 1240 **A.4.2 ABLATION RESULTS**

1241 **Unified model performance.**

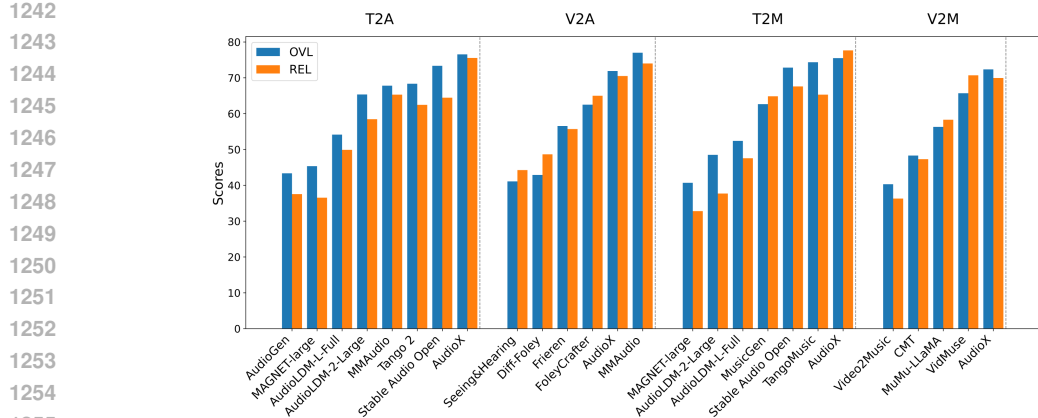


Figure A.2: User study results of generated audio and music. The values represent the average OVL and REL scores across Text-to-Audio (on AudioCaps), Text-to-Music (on MusicCaps), Video-to-Audio (on VGGSound), Video-to-Music (on V2M-bench).

We investigate our unified model’s intra- and inter-modal performance in Fig. A.3. For the intra-modal study, we compare our single unified model against specialist models trained on individual tasks (T2A, V2A, and audio inpainting). The results show our unified model consistently outperforms these specialist models, demonstrating strong intra-modal capabilities. For the inter-modal study on music generation, we find that performance progressively improves as more conditioning modalities are added (e.g., from video-only to video+text). This confirms the model’s robust ability to effectively integrate multiple modalities to enhance generation quality.

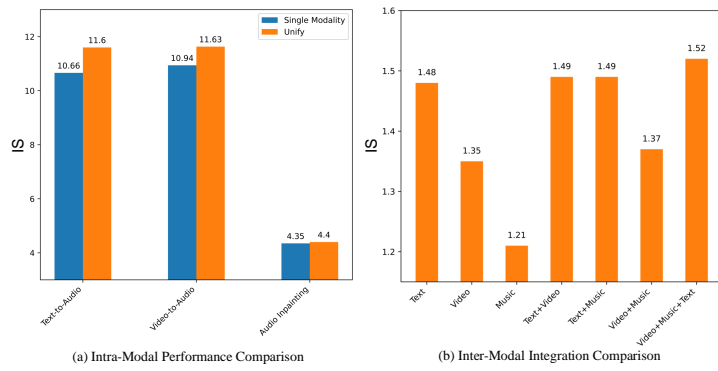
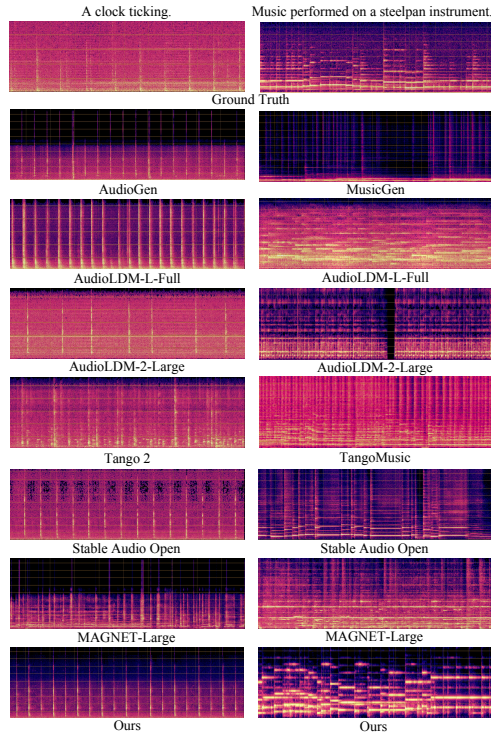


Figure A.3: Ablation study comparing intra-modal and inter-modal performance of the unified model. The left compares single-modality models on text-to-audio, video-to-audio, and audio inpainting tasks. The right shows the effect of adding modalities on music generation, with performance improvements noted for each added modality. Results are based on the Inception Score (IS) metric.

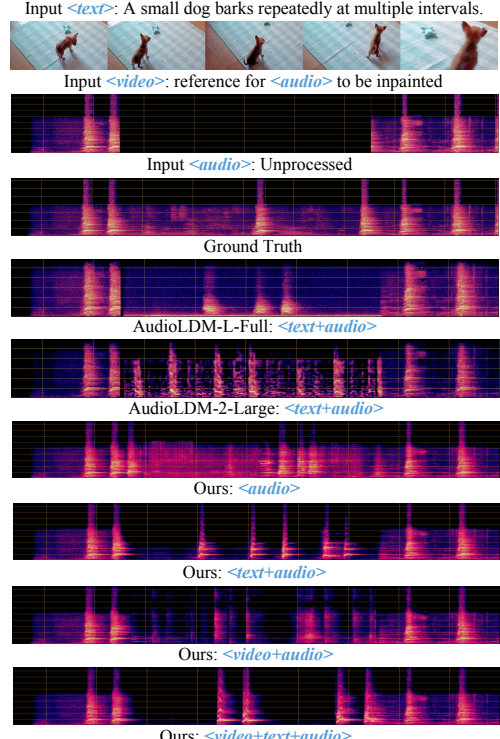
A.5 QUALITATIVE RESULTS

Figures A.4 and A.5 present comprehensive qualitative results.

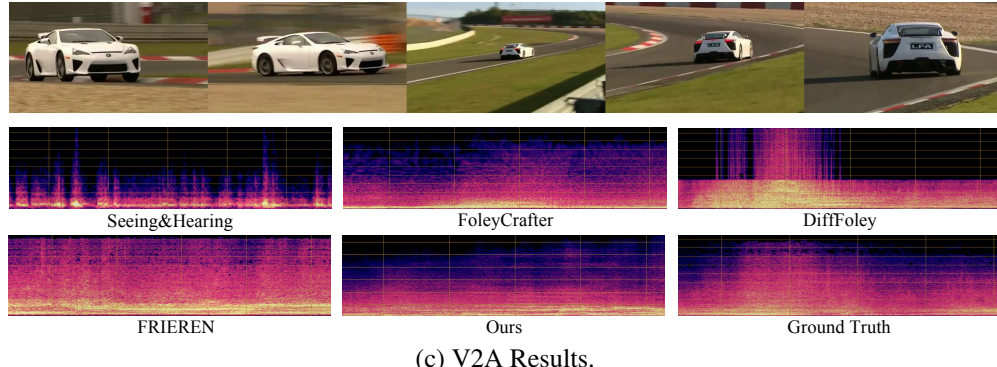
1296
1297
1298
1299
1300



(a) T2A and T2M Results.



(b) Inpainting Results.



(c) V2A Results.

1325
1326
1327
1328
1329
1330
1331
1332
1333
1334
1335
1336
1337
1338
1339
1340
1341
1342
1343
1344
1345
1346
1347
1348
1349

Figure A.4: Qualitative comparison across various tasks: (a) In Text-to-Audio (T2A) and Text-to-Music (T2M) tasks, our model uniquely excels by consistently generating the “ticking” sound of a clock and accurately following the prompt “Music performed on a steelpan instrument,” outperforming baselines in both rhythmic precision and genre fidelity. (b) Audio inpainting results demonstrate our model’s strong context-aware capabilities and its ability to effectively integrate different input modalities. (c) Video-to-Audio (V2A) results show our model’s proficiency in capturing dynamic motion sounds, such as the immersive “drifting” of a car, providing a richer auditory experience compared to baselines.

1350

Text-to-Audio

1351

Text-to-Music

1352

1353

1354

Prompt: A cat meowing twice.

1355

1356

1357

Prompt: A dog is heard continuously barking and whining.

1358

1359

1360

Prompt: The sound is of typing on a computer keyboard.

1361

1362

1363

1364

Prompt: A melody is being played on the violin

1365

1366

(a) Text-to-Audio and Text-to-Music

1367

*Video-to-Audio**Video-to-Music*

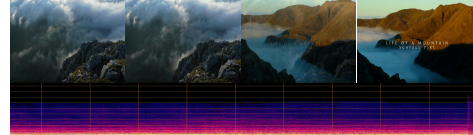
1368

1369

1370

1371

1372



1373

1374

1375

1376

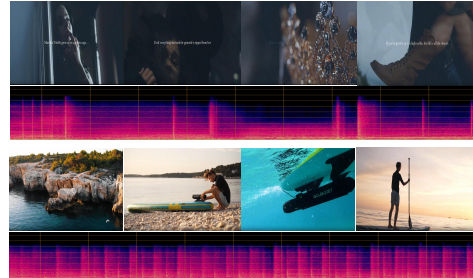
1377

1378

1379

1380

1381



1382

1383

(b) Video-to-Audio and Video-to-Music

1384

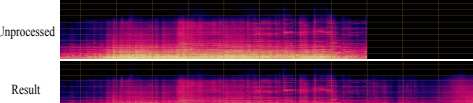
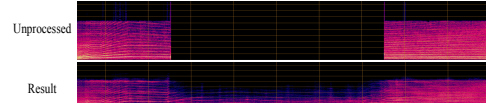
*Audio Inpainting (with text)**Music Completion (with text)*

1385

Prompt: A fire engine horn blows, followed by a fire engine siren blowing.

Prompt: Orchestral, dramatic, epic, intense, powerful, suspenseful, thrilling, cinematic.

1386

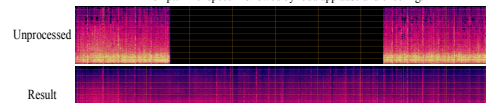


1387

1388

1389

Prompt: Brief speech followed by loud applause and cheering.



1390

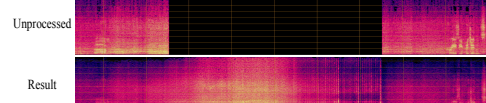
1391

1392

1393

1394

Prompt: Revving of a motorcycle with a man speaking.



1395

1396

1397

1398

1399

1400

1401

1402

1403

(c) Audio Inpainting and Music Completion

Figure A.5: Comprehensive qualitative analysis of our model’s performance across various tasks: (a) Text-to-Audio and Text-to-Music synthesis, (b) Video-to-Audio and Video-to-Music generation, and (c) Audio Inpainting and Music Completion.